JOURNAL OF MATERIALS SCIENCE 35 (2000) 3669–3675

# Piezoresistivity in continuous carbon fiber polymer-matrix and cement-matrix composites

SIHAI WEN, SHOUKAI WANG, D. D. L. CHUNG
*Composite Materials Research Laboratory, State University of New York at Buffalo, Buffalo, NY 14260-4400, USA*
*E-mail: ddlchung@acsu.buffalo.edu*

Piezoresistivity was observed in continuous unidirectional carbon fiber cement-matrix and polymer-matrix composites. The fiber volume fraction was 2.6–7.4% and 58% for cement-matrix and polymer-matrix composites respectively. The DC electrical resistance in the fiber direction increased upon tension in the fiber direction for the cement-matrix composite, due to fiber-matrix interface degradation, but decreased upon tension for the polymer-matrix composite due to increase in the degree of fiber alignment. © *2000 Kluwer Academic Publishers*

## 1. Introduction

Piezoresistivity is a phenomenon in which the electrical resistivity of a material changes with strain, which relates to stress. This phenomenon allows a material to serve as a strain/stress sensor. Applications of the stress/strain sensors include pressure sensors for aircraft and automobile components, vibration sensors for civil structures such as bridges and weighing-in-motion sensors for highways (weighing of vehicles). The first category tends to involve small sensors (e.g., in the form of cement paste or mortar) and they will compete with silicon pressure sensors. The second and third categories tend to involve large sensors (e.g., in the form of precast concrete or mortar) and they will compete with silicon, acoustic, inductive and pneumatic sensors.

Piezoresistivity studies have been mostly conducted on polymer-matrix composites with fillers that are electrically conducting. These composite piezoresistive sensors work because strain changes the proximity between the conducting filler units, thus affecting the electrical resistivity. Tension increases the distance between the filler units, thus increasing the resistivity; compression decreases this distance, thus decreasing the resistivity.

Previously investigated composite piezoresistive materials include polymer-matrix composites containing continuous carbon fibers [1–13], carbon black [14–16], metal particles [15], short carbon fibers [16, 17], cement-matrix composites containing short carbon fibers [18–23], and ceramic-matrix composites containing silicon carbide whiskers [24]. The sensing of reversible strain had been observed in polymer-matrix and cement-matrix composites [1–5, 14, 15, 17–23].

Piezoresistivity in a structural material, such as a continuous fiber polymer-matrix composite, is particularly attractive, since the structural material becomes an intrinsically smart material that senses its own strain without the need for embedded or attached strain sensors. Not needing embedded or attached sensors means lower cost, greater durability, larger sensing volume (with the whole structure being able to sense) and absence of mechanical property degradation (which occurs in the case of embedded sensors).

Piezoresistivity has been previously reported in continuous carbon fiber epoxy-matrix composites [1–13], which are important for lightweight structures. Tensile strain in the fiber direction of a composite results in reversible increase in the resistivity in the through-thickness direction (perpendicular to the fiber layers in the composite) [3, 4], as measured by the four-probe method. This is due to the increase in the degree of fiber alignment and the consequent decreased chance of fibers of adjacent layers touching one another. Tensile strain in the fiber direction also results in reversible decrease in the resistance in the fiber direction, as measured by using the four-probe method in which two current (outer) and two voltage (inner) contacts are around the entire perimeter of the composite at four planes that are perpendicular to the fiber direction [1, 2, 4]. This was attributed to the increase in the degree of fiber alignment [1, 2, 4], just as the phenomenon observed in the through-thickness direction. However, by using the two-probe method in which the common current/voltage contacts are at the ends of the fibers in the composite, the resistance in the fiber direction was observed to increase upon tension in the fiber direction [5–12]. Ref. 5 further reported that the resistance increase was reversible and attributed this phenomenon to the dimensional changes during tension.

The opposite trends described above in the change in resistance in the fiber direction upon tensile strain in the fiber direction are due to the difference in electrical contact configurations, so a study of the effect of electrical contact configuration is needed. The four-probe method [1, 2, 4] is in general better than the two-probe method [5–12], due to the elimination of the contact resistance from the measured resistance. Moreover, practical implementation of strain sensing (particularly

strain distribution sensing) is more convenient when the contacts do not have to be at the ends of the fibers. However, having the current contacts at the ends of the fibers [5–12] ensures that current goes through all the fibers. Therefore, this paper provides a systematic comparison of the results obtained on the same composite with four contact configurations, namely (i) four-probe method with all four contacts around the entire perimeter at four planes that are perpendicular to the fiber direction, (ii) four-probe method with two voltage contacts around the entire perimeter at two planes that are perpendicular to the fiber direction and two current contacts at the fiber ends, (iii) two-probe method with both contacts around the entire perimeter at two planes that are perpendicular to the fiber direction, and (iv) two-probe method with both contacts at the fiber ends.

Due to the electrical conductivity of carbon fibers and the slight conductivity of the cement matrix, measurement of the DC electrical resistance of a carbon fiber cement-matrix composite provides a way to detect damage. Fiber breakage obviously causes the longitudinal resistance to increase irreversibly. Fiber-matrix bond degradation obviously increases the transverse resistance, but it also increases the longitudinal resistance when the electrical current contacts are on the surface (e.g., perimetrically around the composite in a plane perpendicular to the longitudinal direction). When the transverse resistivity is increased, the electrical current has more difficulty in penetrating the entire cross-section of the specimen, thereby resulting in an increase in the measured longitudinal resistance. Note that the electrical resistivity of carbon fibers is $10^{-4}$ Ω·cm, whereas that of cement paste is $10^{5}$ Ω·cm.

Although piezoresistivity has been reported in short fiber cement-matrix composites, it has not been previously reported in continuous fiber cement-matrix composites. This paper addresses piezoresistivity in continuous carbon fiber cement-matrix and polymer-matrix composites.

## 2. Polymer-matrix composites

### 2.1. Experimental methods

The composite materials used are the same as those used in Ref. 2. They were constructed from individual layers cut from a 12 inch wide unidirectional carbon fiber prepreg tape manufactured by ICI Fiberite (Tempe, AZ). The product used was Hy-E 1076E, which consisted of a 976 epoxy matrix and 10E carbon fibers. The fiber and matrix properties are shown in Table I. The matrix was electrically insulating, whereas the fibers were electrically conducting, with a resistivity of $2.2 \times 10^{-3}$ Ω·cm.

The composite laminates were laid up in a 4 inch × 7 inch platen compression mold with laminate configuration $[0]_8$ (i.e., eight unidirectional fiber layers in the laminate). The individual 4 inch × 7 inch fiber layers were cut from the prepreg tape. The layers were stacked in the mold with a mold release film on the top and bottom of the layup. No liquid mold release was necessary. The density and thickness of the laminate were $1.52 \pm 0.01$ g cm$^{-3}$ and 1.1 mm respectively. The volume fraction of carbon fibers in the composite was 58%.

TABLE I Carbon fiber and epoxy matrix properties (according to ICI Fiberite)

| | |
|---|---|
| 10E–Torayca T-300 (6K) untwisted, UC-309 sized | |
| Diameter | 7 μm |
| Density | 1.76 g cm$^{-3}$ |
| Electrical resistivity | $2.2 \times 10^{-3}$ Ω·cm |
| Tensile modulus | 221 GPa |
| Tensile strength | 3.1 GPa |
| 976 epoxy | |
| Process temperature | 350°F (177°C) |
| Maximum service temperature | 350°F (177°C) dry<br>250°F (121°C) wet |
| Flexural modulus | 3.7 GPa |
| Flexural strength | 138 MPa |
| $T_g$ | 232°C |
| Density | 1.28 g cm$^{-3}$ |

The volume resistivity of the laminate in the fiber direction was $4.1 \times 10^{-3}$ Ω·cm, as measured by the four-probe method and silver paint electrical contacts around the perimeter of the sample at four planes perpendicular to the fiber direction. The resistivity calculated by using the Rule of Mixtures was $3.8 \times 10^{-3}$ Ω·cm. That the measured resistivity was higher than the calculated value is attributed to the limited degree of fiber alignment. The laminates were cured using a cycle based on the ICI Fiberite C-5 cure cycle. Curing occurred at $355 \pm 10$°F ($179 \pm 6$°C) and 89 psi (0.61 MPa) for 120 min. Afterward, they were cut to pieces of size $176 \times 8.9 \times 1.1$ mm. Glass fiber reinforced epoxy end tabs for gripping the sample during subsequent tension were applied to both ends on both sides of each piece, such that the inner edges of the end tabs on the same side were 100 mm apart.

The electrical resistance $R$ was measured in the fiber (longitudinal) direction while cyclic tension was applied in the same direction. Silver paint was used for electrical contacts.

In the four-probe method, the four probes consisted of two outer current probes and two inner voltage probes. The measured resistance is the sample resistance between the inner probes. In one four-probe contact configuration [2], the four electrical contacts were around the whole perimeter of the sample in four parallel planes that were perpendicular to the fiber direction, such that the inner probes were 45 mm apart. In another four-probe configuration, the current probes were at the end faces containing the fiber ends, such that these faces were flush with the outer edges of the end tabs and the current contacts were not gripped during subsequent tensile testing, while the voltage probes were the same as those in the other four-probe configuration.

In one two-probe configuration, the two contacts were at the end faces containing the fiber ends, such that these faces were flush with the outer edges of the end tabs and the current contacts were not gripped during subsequent tensile testing. Although separate wires were used for the current and voltage probes, they were electrically connected to the same point on the sample. Hence, the two-probe method was used in spite of the presence of four wires. This two-probe method was also used in Ref. 5, although Ref. 5 referred to it as the four-probe method. In the other two-probe configuration

of this work, the two contacts were around the whole perimeter of the sample in four parallel planes that were perpendicular to the fiber direction, such that the contacts were 45 mm apart. In either two-probe configuration, each of these two contacts served as both current and voltage contacts, though separate wires were used for passing current and for voltage measurement at each contact in order to eliminate the resistance of the wires from the measured resistance.

A strain gage was attached to the center of one of the largest opposite faces. A Keithley 2001 multimeter was used for DC resistance measurement. The displacement rate was 0.5 mm $min^{-1}$. A hydraulic mechanical testing system (MTS 810) was used for cyclic tensile loading in the fiber direction.

## 2.2. Results and discussion

Fig. 1 shows the change in resistance during cyclic tension for the four-probe configuration in which all contacts were around the whole perimeter of the sample in four parallel planes that were perpendicular to the fiber direction. The resistance decreased reversibly upon tension, as in Ref. 2. The gage factor (fractional reversible change in resistance per unit strain) was −22. Fig. 2 shows the corresponding result for the other four-probe configuration, in which the current contacts were at the fiber ends and the voltage contacts were around the whole perimeter of the sample in two parallel planes that were perpendicular to the fiber direction. The resistance decreased vertically upon tension, as in Fig. 1, but the gage factor was only −3.8, the resistance was smaller (resistance before loading = 0.206 Ω in Fig. 2, but was 0.243 Ω in Fig. 1) and the resistance change upon loading was more noisy. The higher resistance in Fig. 1 is attributed to the perimetric current contacts of Fig. 1 being not able to get the current to penetrate the entire cross-section of the sample evenly, whereas the current contacts at the fiber ends (Fig. 2) ensured current penetration throughout the sample cross section.

For both two-probe configurations (Figs 3 and 4), the resistance increased upon tension, in contrast to the opposite trend for both four-probe configurations (Figs 1 and 2). The resistance before loading was 0.774 Ω for Fig. 3 (perimetric contacts) and 6.79 Ω for Fig. 4 (contacts at fiber ends). This means that the resistance of the contacts at the fiber ends was much higher than that of the perimetric contacts. The noisiness and the low magnitude of the gage factor in Fig. 2 compared to Fig. 1

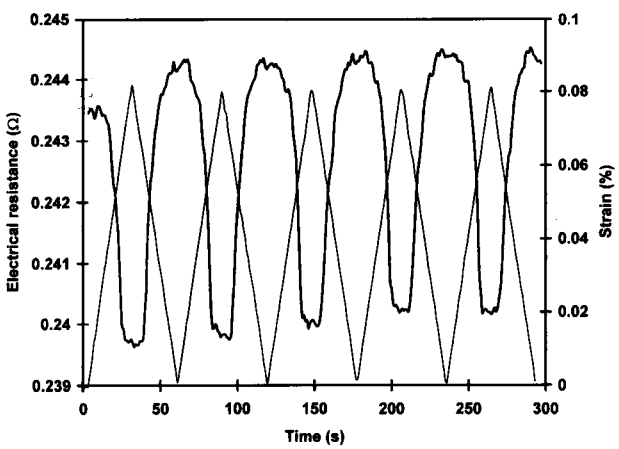


*Figure 1* Plots of resistance (four-probe method with all four contacts perimetric) vs. time and of strain vs. time during cyclic tension. Resistance: thick line. Strain: thin line.

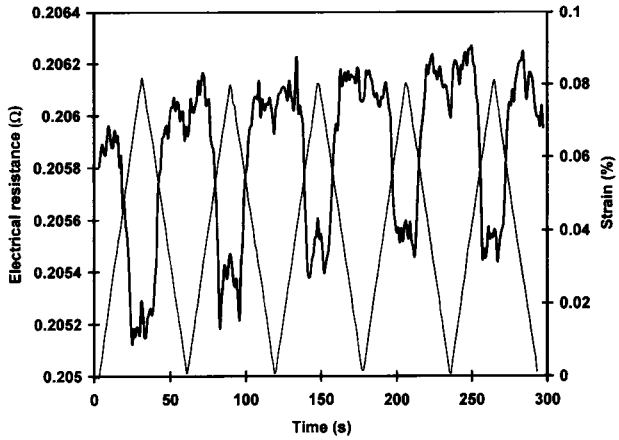


*Figure 2* Plots of resistance (four-probe method with two voltage contacts perimetric and two current contacts at the fiber ends) vs. time and of strain vs. time during cyclic tension. Resistance: thick line. Strain: thin line.

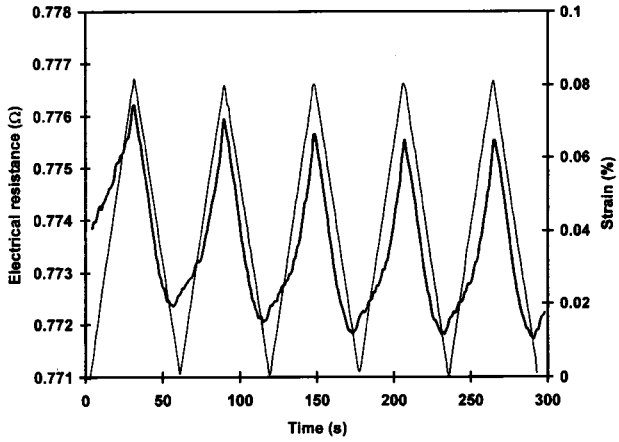


*Figure 3* Plots of resistance (two-probe method with contacts perimetric) vs. time and of strain vs. time during cyclic tension. Resistance: thick line. Strain: thin line.

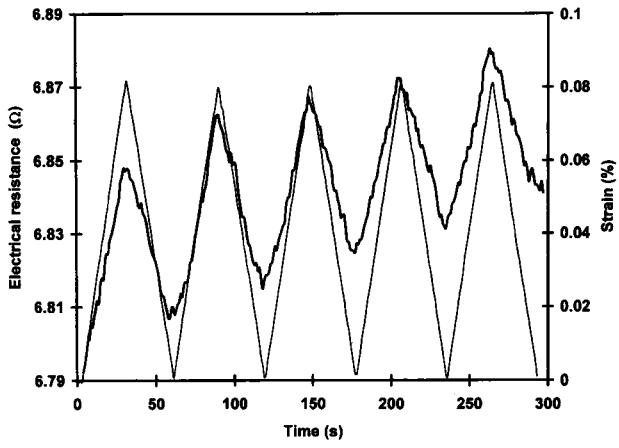


*Figure 4* Plots of resistance (two-probe method with contacts at the fiber ends) and of strain vs. time during cyclic tension. Resistance: thick line. Strain: thin line.

are attributed to the high resistance of the contacts at the fiber ends compared to that of the perimetric contacts. This is because perimetric contacts can be secured by twisting the wires, but this cannot be done for the contacts at the fiber ends.

Based on the resistivity of the composite in the fiber direction ($4.1 \times 10^{-3}$ Ω·cm), the volume resistance of the whole sample of Fig. 4 in the fiber direction was calculated to be 0.74 Ω. This means that the high resistance in Fig. 4 is almost all due to the contact resistance. Based on the resistivity of the composite, the volume resistance of the sample of Figs 1–3 between the voltage probes (45 mm apart) was calculated to be 0.19 Ω. This means that the resistance in Figs 1 and 2 is essentially the volume resistance of the sample and the resistance in Fig. 3 is dominated by the contact resistance. Hence, the four-probe method (Figs 1 and 2) yields the volume resistance, whereas the two-probe method (Figs 3 and 4) yields mainly the contact resistance.

That the resistance before loading was much lower in Fig. 1 than Fig. 3 means that the resistance in Fig. 3 was dominated by the contact resistance. That the resistance before loading was very much lower in Fig. 2 than Fig. 4 means that the resistance in Fig. 4 was much dominated by the contact resistance. That the resistance increased upon tension in Figs 3 and 4 is attributed to the contact resistance increasing (i.e., contacts degrading) upon tension. The gage factor was +5.5 and +9.6 for Figs 3 and 4 respectively. The higher gage factor in Fig. 4 compared to Fig. 3 is attributed to the greater dominance of the contact resistance in Fig. 4 than in Fig. 3. The resistance change upon loading was more noisy in Fig. 4 than Fig. 3, due to the noise associated with changes in the quality of the contacts at the fiber ends. The reason is similar to that for the greater noisiness in Fig. 2 than in Fig. 1.

The stress (not shown in Figs 1–4) was linear with strain, such that the strain was totally reversible and was 0.08% at a stress of 140 MPa.

The resistance increase upon tension in Fig. 4 cannot be just due to dimensional changes (in contrast to the claim in Ref. 5), since the gage factor would have been only +2 if that were the case. The observed large gage factor of +9.6 for Fig. 4 is attributed to the degradation of the electrical contacts during tension and the consequent increase in contact resistance. Although the contacts at the fiber ends were not gripped during tension, slight pull-out of the fibers away from the contact and into the composite probably occurred during tensile loading of the composite, thereby resulting in electrical contact degradation (i.e., contact resistivity increase). This degradation is reversible, as shown by the reversibility of the resistance increase (Fig. 4), due to the reversibility of the contact degradation mechanism. Because the resistance increase in Figs 3 and 4 is not due to a change in volume resistivity, but a change in contact resistivity, the phenomenon of Figs 3 and 4 is not true piezoresistivity.

Although the phenomenon of Figs 3 and 4 is not true piezoresistivity, it is still an electromechanical effect. However, this effect is not suitable for use in strain sensing, because the quality of an electrical contact is hard to control in practice (especially in a real structure) and the gage factor associated with this phenomenon depends on the contact quality, which is reflected by the contact resistance before loading.

The resistance decrease upon tension in Figs 1 and 2 is attributed to the increase in the degree of fiber alignment [1, 2, 4] (as supported by the concurrent increase in through-thickness resistance [3]), although the exact mechanism is unclear. This interpretation is consistent with the fact that the measured resistivity of the composite in the fiber direction is higher than that calculated by using the Rule of Mixtures. Note that the resistance decrease upon tension cannot be due to an increase in the depth of current penetration, since the through-thickness resistance increases upon tension. An increase in the degree of fiber alignment is expected to decrease the resistivity, because the misaligned fibers may not be at the same potential as the aligned fibers at the same cross-sectional plane perpendicular to the current direction, so that the misaligned fibers may contribute less to conduction than the aligned fibers.

The two-probe method is simpler to implement than the four-probe method. However, the two-probe method and the four-probe method measure different quantities. Therefore, for use of the composite as a strain sensor, the four-probe method is necessary.

## 3. Cement-matrix composites

### 3.1. Experimental methods

The continuous carbon fibers used were pitch-based, Thornel P-25, 2000 fibers per tow, without sizing, without twist, from Amoco Performance Products, Inc., Ridgefield, CT. The fiber properties are shown in Table II. Prior to using the fibers in cement, they were dried at 110°C in air for 1 h and then surface treated with ozone by exposure to $O_3$ gas (0.6 vol. %, in $O_2$) at 160°C for 10 min. The ozone treatment is for improving the wetting of the fibers by water [25]. Cement paste made from portland cement (Type I) from Lafarge Corp. (Southfield, MI) was used for the cementitious material.

Water and cement in the weight ratio 0.45 were mixed by hand to form a cement paste. A weighed amount of continuous carbon fiber tow was immersed in the cement paste for 60 min in order to impregnate the fiber tow with cement paste. After this, the fiber tow was taken out and a fraction of the cement paste on the outer surface of the tow was removed by using tweezers. Then, for the purpose of straightening the tow, the tow was stretched and wound around a glass cylinder of diameter 12 cm and allowed to remain wound for 7–10 min. After this, the tow was unwound and cut into 180 mm lengths. Then the cut lengths were laid one by one into the rectangular cavity of a steel mold (Fig. 5)

TABLE II Fiber properties

| | |
|---|---|
| Tensile strength | 1.40 GPa |
| Tensile modulus | 160 GPa |
| Elongation at break | 0.90% |
| Electrical resistivity | $1.3 \times 10^{-4}$ Ω·cm |
| Density | 1.9 g/cm$^3$ |
| Diameter | 11 $\mu$m |

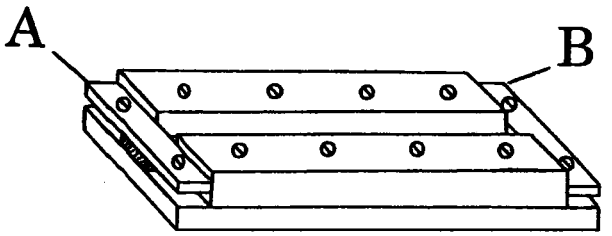


*Figure 5* Steel mold for specimen preparation. The piston above the mold cavity is not shown. The impregnated fiber tows (dotted region corresponding to the fiber ends) are in the cavity and are fastened at both ends by small steel plates A and B. The circles are screws for fastening.

and the ends of each tow were fastened through small steel plates at the ends of the mold. The inner edges of the small steel plates were 150 mm apart, thus forming a mold cavity that was 150 mm long and 14 mm wide. A steel piston of the size of the cavity was then lowered into the cavity. A pressure of 32 MPa was applied to the cavity through the piston. After holding the pressure for 24 h, demolding took place and curing was performed at 100% relative humidity for 7 days. After this, the specimen was dried at 50°C for 1 h. Then the specimen was weighed. The previously determined weight of the bare carbon fibers divided by the weight of the specimen gave the weight fraction of fibers in the specimen. Using the density of the fibers (Table II), the weight fraction was converted to volume fraction. After this, the specimen was cut and mechanically polished to size 150 × 12 × 5 mm for tensile testing. Specimens with different fiber contents (Table III) were obtained by varying the amount of cement paste that was removed by tweezers from the impregnated fiber tow. Six specimens of each fiber content were prepared and tested. Among the six, three were for static loading and the other three were for repeated loading.

The DC electrical resistance in the stress direction was measured during tensile testing. For the resistance measurement, a Keithley 2002 multimeter and the four-probe method were used. In this method, four electrical contacts were applied by silver paint around the whole perimeter at four planes perpendicular to the length of the specimen. The four planes were symmetrical around the mid-point along the length of the specimen, such that the two outer contacts (for passing current) were 70 mm apart and the two inner contacts (for measuring voltage) were 50 mm apart.

In order to facilitate the gripping of the specimens during tensile testing, glass fiber epoxy-matrix composite end caps were adhesively applied to the ends (15 mm length at each end) of each specimen. The stress direction during tensile testing was along the length of the specimen. The strain in the stress direction during tensile testing was measured by using a strain gage, which was attached to the mid-point along the length of the specimen, i.e., between the two inner electrical contacts. Tensile testing under load control was performed using a hydraulic mechanical testing system (MTS Model 810). Testing was conducted under static loading up to failure and under repeated loading at various stress amplitudes, which correspond to load amplitudes of 50, 100 and 150 lb. The loading rate was 2.45–6.25 lb/s for static loading and 0.125–0.375 lb/s for repeated loading.

## 3.2. Results

Fig. 6 shows the relationship between stress and strain and that between fractional resistance change ($\Delta R/R_0$) and strain during static tensile testing up to failure for a composite with 2.57 vol. % carbon fibers. The stress-strain curve was linear up to a strain of 0.2%, at which the resistance started to increase abruptly. Fig. 7 shows the variation of $\Delta R/R_0$ during loading and unloading for various stress amplitudes within the linear portion of the stress-strain curve for a specimen with essentially the same fiber content. The resistance increased upon loading and decreased upon unloading in every cycle, such that the resistance increase was not totally reversible. The gage factor, which is the fractional change in resistance (reversible portion) per unit strain, is 28, 21 and 17 for the first, second and third cycles respectively (Fig. 7). The decrease in gage factor with increasing cycle number (increasing stress amplitude) was observed

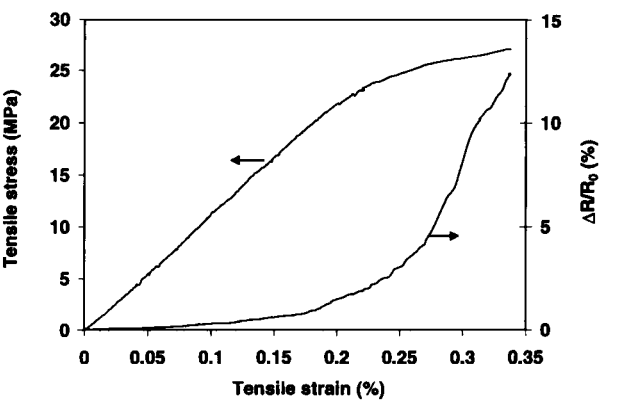


*Figure 6* Relationship between stress and strain and that between fractional resistance change ($\Delta R/R_0$) and strain during static tensile testing up to failure for a cement-matrix composite with 2.57 vol. % carbon fibers.

TABLE III Fiber content and density

| Fiber content | | | | | |
|---|---|---|---|---|---|
| Weight fraction (%) | | Volume fraction (%) | | Density (g/cm$^3$) | |
| Static loading | Repeated loading | Static loading | Repeated loading | Static loading | Repeated loading |
| 2.20 ± 0.21 | 2.24 ± 0.14 | 2.57 ± 0.42 | 2.60 ± 0.06 | 2.23 ± 0.15 | 2.21 ± 0.09 |
| 4.61 ± 0.74 | 4.55 ± 0.44 | 5.19 ± 1.35 | 5.14 ± 0.25 | 2.16 ± 0.21 | 2.15 ± 0.13 |
| 7.02 ± 0.69 | 6.67 ± 0.43 | 7.37 ± 1.17 | 7.24 ± 0.24 | 2.00 ± 0.12 | 2.06 ± 0.05 |

TABLE IV Gage factor

| Cycle No. | Maximum load (lb) | Fiber volume fraction (%) 2.60 ± 0.06 | 5.14 ± 0.25 | 7.24 ± 0.24 |
|---|---|---|---|---|
| 1 | 50 | 32.6 ± 7.9 | 57.6 ± 2.8 | 33.7 ± 6.5 |
| 2 | 100 | 24.6 ± 6.9 | 41.7 ± 2.6 | 24.0 ± 2.0 |
| 3 | 150 | 16.3 ± 1.3 | 40.9 ± 1.7 | 23.4 ± 3.6 |

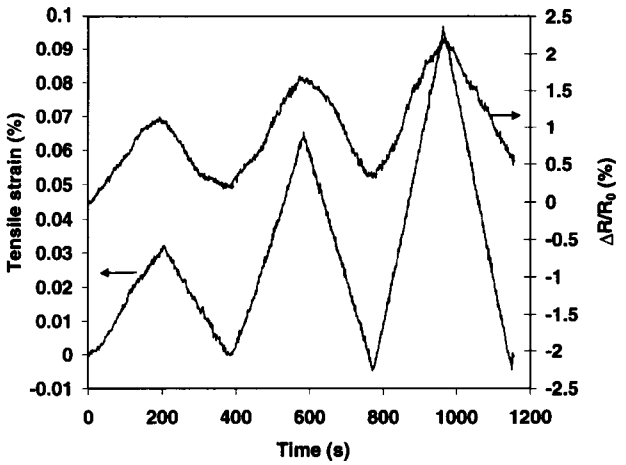


*Figure 7* Variation of $\Delta R/R_0$ during loading and unloading for various stress amplitudes within the linear portion of the stress-strain curve for a cement-matrix composite with 2.60 vol. % carbon fibers.

in all samples (Table IV). It is attributed to the decrease in reversibility with increasing stress amplitude. It is not clear why the intermediate fiber volume fraction gave the highest gage factor. Investigation of composites with different fiber contents showed that the extent of irreversibility in resistance increase was greater when the stress amplitude as a fraction of the tensile strength was higher.

Similar piezoresistive behavior was observed for composites with various fiber contents. Table V lists the tensile properties and resistivity of composites with various fiber contents. The tensile strength and modulus approach the values calculated based on the Rule of Mixtures. The resistivity is higher than that calculated from the Rule of Mixtures. The ductility, strength and modulus all increase with increasing fiber volume fraction.

## 3.3. Discussion

The abrupt increase in resistance at high strains is accompanied by a decrease in modulus (Fig. 6), so it is attributed to fiber breakage. The smaller increase in resistance at low strains is not accompanied by any change in modulus (Fig. 6), so it is attributed to fiber-matrix interface degradation. The degradation causes the fiber-matrix contact resistivity to increase, thereby affecting the measured resistance, as explained in the Introduction. Fig. 7 shows that the resistance increase due to fiber-matrix interface degradation is mostly reversible. The large gage factor means that the resistance increase cannot be explained by the dimensional change, which would have resulted in a gage factor of 2 only. The partly reversible fiber-matrix interface degradation probably involves reversible slight loosening of the interface. The irreversible part of the resistance increase is associated with irreversible degradation of the interface. The reversibility is consistent with that observed in short carbon fiber cement-matrix composites [18–23]. The reversible resistance change means that the continuous carbon fiber composites are strain sensors. The mechanisms of reversible resistance increase is fiber-matrix interface loosening for both short fiber and continuous fiber composites. However, the gage factor is much higher for short fiber than continuous fiber composites.

Since a broken fiber acts as an open circuit, the increase in resistance in the regime of static testing associated with fiber breakage yields the fraction of fibers broken, as shown in Fig. 8 for the sample of Fig. 6. At

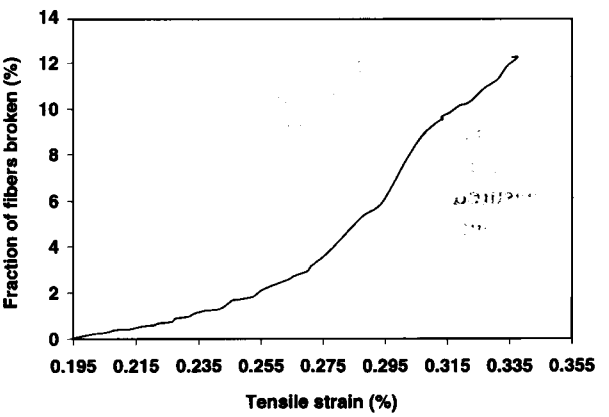


*Figure 8* Fraction of fibers broken vs. tensile strain, as obtained from Fig. 6.

TABLE V Tensile properties and electrical resistivity

| | Carbon fiber volume fraction (%) 2.57 ± 0.42 | 5.19 ± 1.35 | 7.37 ± 1.17 |
|---|---|---|---|
| Tensile strength (MPa) | | | |
| Measured | 27.2 ± 1.2 | 57.3 ± 1.1 | 85.7 ± 1.32 |
| Calculated* | 30.8 | 64.4 | 98 |
| Tensile modulus (GPa) | | | |
| Measured | 11.1 ± 0.52 | 14.6 ± 0.86 | 17.3 ± 0.92 |
| Calculated* | 13.1 | 17.1 | 20.8 |
| Ductility (%) | 0.341 ± 0.011 | 0.468 ± 0.008 | 0.485 ± 0.008 |
| Resistivity (Ω·cm) | | | |
| Measured | $(1.10 \pm 0.11) \times 10^{-1}$ | $(8.40 \pm 0.94) \times 10^{-2}$ | $(4.56 \pm 1.32) \times 10^{-2}$ |
| Calculated* | $5.91 \times 10^{-2}$ | $2.83 \times 10^{-2}$ | $1.86 \times 10^{-2}$ |

*Based on the Rule of Mixtures.

failure, 12% of the fibers were broken. This fraction is similarly low for continuous carbon fiber epoxy-matrix composites [4].

The method of composite fabrication in this work involved impregnation followed by curing of the impregnated fiber tows under slight tension. Saito *et al.* [26] involved impregnation followed by lay-up of the impregnated tows without tension. Our composites exhibit tensile strength equal to $(88 \pm 1)\%$ of the calculated value based on the Rule of Mixtures, whereas those of Ref. 26 exhibit tensile strength equal to 75% of the calculated value. We have made composites without tension on the impregnated fiber tows. The resulting composites are poor in strength and modulus due to the poor alignment of the fibers.

In spite of the effort to align the fibers in this work, the fiber alignment is still not perfect, as shown by the low strength, low modulus and high resistivity relative to the calculated values (Table V). Nevertheless, the tensile strength, which reaches 86 MPa, makes these composites attractive for structural applications related to tension members, repair, surface strengthening and lightweight structures.

Using the same four-probe method involving four perimetric electrical contacts, the resistance of the epoxy-matrix composites in the fiber direction decreases upon tension in the fiber direction, whereas that of the cement-matrix composites increases upon tension in the fiber direction. This difference in behavior is due to the difference in mechanism. The resistance decrease in the epoxy-matrix composites is due to the increase in the degree of fiber alignment, whereas that in the cement-matrix composites is due to the fiber-matrix interface degradation. The fiber-matrix bond is much stronger for epoxy than cement and the fiber content is much higher for epoxy-matrix than cement-matrix composites. Moreover, epoxy is much more ductile than cement under tension. These differences in characteristics between epoxy and cement probably cause the difference in piezoresistive behavior.

## 4. Conclusion

Piezoresistivity in continuous unidirectional carbon fiber epoxy-matrix composites was observed upon tension in the fiber direction. The phenomenon involved the volume resistivity of the composite in the fiber direction decreasing reversibly upon tension, due to an increase in the degree of fiber alignment, as observed by using the four-probe method. Use of the two-probe method resulted in measurement of the contact resistance rather than the volume resistance. The contact resistivity increased reversibly upon tension, but the phenomenon is not true piezoresistivity and is not suitable for practical use for strain sensing due to the need to have the electrical contacts at the fiber ends.

Piezoresistivity with gage factor up to +60 was observed in continuous carbon fiber cement-matrix composites with fiber volume fractions in the range from 2.6 to 7.4%. The electrical resistance in the fiber direction, as measured using surface electrical contacts, increases upon tension in the same direction. The resistance increase is mostly reversible, such that the irreversible portion increases with the stress amplitude. The effect is attributed to fiber-matrix interface degradation, which is partly irreversible. At higher strains at which the modulus is decreased, the resistance increases with strain abruptly, due to fiber breakage. The tensile strength of the composites is $(88 \pm 1)\%$ of the calculated value based on the Rule of Mixtures. The tensile modulus $(84 \pm 1)\%$ of the calculated value based on the Rule of Mixtures.


## Acknowledgement

This work was supported in part by the National Science Foundation. The authors thank Xiaojun Wang of State University of New York at Buffalo for technical assistance.


## References


1. X. WANG and D. D. L. CHUNG, *Smart Mater. Struct.* **5** (1996) 796.
2. *idem., ibid.* **6** (1997) 504.
3. *idem., Polymer Composites* **18**(6) (1997) 692.
4. *idem., Composites: Part B* **29B**(1) (1998) 63.
5. P. E. IRVING and C. THIAGARAJAN, *Smart Mater. Struct.* **7** (1998) 456.
6. N. MUTO, H. YANAGIDA, T. NAKATSUJI, M. SUGITA, Y. OHTSUKA, Y. ARAI and C. SAITO, *Adv. Composite Mater.* **4**(4) (1995) 297.
7. M. SUGITA, H. YANAGIDA and N. MUTO, *Smart Mater. Struct.* **4**(1A) (1995) A52.
8. R. PRABHAKARAN, *Experimental Techniques* **14**(1) (1990) 16.
9. K. SCHULTE and CH. BARON, *Composites Sci. Tech.* **36** (1989) 63.
10. K. SCHULTE, *J. Physique IV, Colloque C7* **3** (1993) 1629.
11. O. CEYSSON, M. SALVIA and L. VINCENT, *Scripta Materialia* **34**(8) (1996) 1273.
12. J. C. ABRY, S. BOCHARD, A. CHATEAUMINOIS, M. SALVIA and G. GIRAUD, *Composites Sci. Tech.* **59**(6) (1999) 925.
13. A. S. KADDOUR, F. A. R. AL-SALEHI, S. T. S. AL-HASSANI and M. J. HINTON, *ibid.* **51**(3) (1994) 377.
14. J. KOST, M. NARKIS and A. FOUX, *J. Appl. Polymer Science* **29** (1984) 3937.
15. S. RADHAKRISHNAN, SANJAY CHAKNE and P. N. SHELKE, *Mater. Lett.* **18** (1994) 358.
16. P. K. PRAMANIK, D. KHASTGIR, S. K. DE and T. N. SAHA, *J. Mat. Sci.* **25** (1990) 3848.
17. M. TAYA, W. J. KIM and K. ONO, *Mechanics of Materials* **28**(1/4) (1998) 53.
18. P. CHEN and D. D. L. CHUNG, *Smart Mater. Struct.* **2** (1993) 22.
19. *Idem., Composites, Part B* **27B** (1996) 11.
20. *Idem., ACI Mater. J.* **93**(4) (1996) 341.
21. X. FU and D. D. L. CHUNG, *Cem. Conc. Res.* **26**(1) (1996) 15.
22. X. FU, E. MA, D. D. L. CHUNG and W. A. ANDERSON, *Cem. Concr. Res.* **27**(6) (1997) 845.
23. X. FU, W. LU and D. D. L. CHUNG, *ibid.* **28**(2) (1998) 183.
24. A. ISHIDA, M. MIYAYAMA and H. YANAGIDA, *J. Am. Ceramic Soc.* **77**(4) (1994) 1057.
25. X. FU, W. LU and D. D. L. CHUNG, *Carbon* **36**(9) (1998) 1337.
26. K. SAITO, N. KAWAMURA and Y. KOGO, in 21st Int. SAMPE Technical Conf., 1989, p. 796.



*Received 2 February*
*and accepted 22 December 1999*